Absolute Equation of State Measurements of Compressed Liquid Deuterium Using Nova

R. Cauble
L. B. Da Silva
P. Celliers
G. W. Collins
K. S. Budil
N. C. Holmes
B. A. Hammel
J. D. Kilkenny
R. J. Wallace
*A. Ng**

Introduction

The equations of state (EOSs) of hydrogen and its isotopes at high pressure are essential components of the physics of high-density matter.[1,2] For example, the internal structure of Jovian planets is very sensitive to and largely determined by the hydrogen EOS in the pressure range of 1.0 Mbar to 10.0 Mbar.[3] Further, the performance of deuterated inertial confinement fusion (ICF) capsules relies on shock timing and efficient compression, which are critically dependent on the EOSs.[4] In ICF, a "softer," or more compressible, EOS of the deuterium–tritium (DT) fuel is advantageous for ignition. For these reasons, a number of theoretical models of the EOS of hydrogen have been proposed.[5–7]

An important question in the EOS of H_2, as well as of D_2, has been the transition from a diatomic to a monatomic fluid. A continuous dissociative transition has been suspected, but theoretical predictions of molecular dissociation have been complicated by the presence of electronic transitions and possible ionization near pressures required for dissociation (~1.0 Mbar).[8] In spite of the expected simplicity of the element, there is no inclusive theory for a strongly coupled mixture of hydrogen ions, atoms, and molecules. In the following, we describe results of the first measurements of the principal Hugoniot (i.e., a curve in the EOS that will be defined subsequently) of liquid deuterium compressed with pressures as great as 2.1 Mbar. These absolute EOS data reveal a substantially enhanced compressibility that is an indicator of dissociation.

* University of British Columbia, Vancouver, B. C., Canada.

High-Pressure Hydrogen EOS and ICF

The EOS of the hydrogen-isotope fuel governs the reaction of an ICF capsule to outside pressures to compress the capsule. The fuel must be highly compressed in order to ignite.[4] To reach a high final density, the fuel must be compressed without excessive heating because the more internal energy the fuel has, the more difficult it is to compress and confine it. To compress ICF capsules without excessive heat, a series of progressively stronger shocks is envisioned. In the point-design ignition capsule to be used for the National Ignition Facility (NIF), three main shocks are used, the first of which is delivered to the DT fuel at 0.9 Mbar.[9]

It has been shown that the more compressible the hydrogen EOS is at this pressure, the higher will be the expected yield from the capsule[10] (a greater compressibility means a higher density of the fuel at a given pressure). The higher yield is primarily the result of the capsule fuel's higher final density when the fuel ignites. It is also due to a lower predicted Rayleigh–Taylor instability growth rate. Additionally, the greater the compressibility of the EOS, the less sensitive the calculated yield is to the exact pressure of the first shock.

Molecular dissociation of deuterium can be a source of enhanced compressibility and has been expected to occur in the pressure regime near 1.0 Mbar. Dissociation is an energy sink (it takes energy to break the molecular bonds), so some of the energy transmitted to the NIF capsule fuel from the first shock will be used for this process. The more energy required for dissociation, the lower the temperature of the shocked fluid and, consequently,

the higher the shocked density. The experiments described subsequently were undertaken to evaluate compressionof liquid deuterium in the 1.0-Mbar pressure regime.[11]

EOS data for hydrogen in the pressure regime greater than 0.1 Mbar have been obtained by dynamic shock compression and by static compression in diamond-anvil cells. The latter method is used to study static, isothermal properties of solid hydrogen at pressures as great as 3.0 Mbar at very low temperatures.[12] Shock compression produces higher temperatures than does static compression. In shock compression, the most accurate data have been produced using light gas guns.[13–15] While both methods access equilibrium states of matter, the final-state densities and temperatures obtained by shock compression are directly applicable to ICF.

Shock-wave experiments are the only practical technique for measuring high-pressure EOSs. The final state of a shocked material is simply related to the initial state through the Hugoniot relations. These relations are derived by applying conservation equations across the shock front. Conservation relations require that two independent parameters be measured to obtain an *absolute* EOS data point (nonabsolute comparative data are often used to assess the EOS of one material with respect to another). The shock speed U_s, the particle (or pusher) speed U_p, the pressure P, and the final density ρ are related by

$$P - P_0 = \rho_0 U_s U_p \quad (1)$$

and

$$\rho/\rho_0 = U_s/(U_s - U_p) \quad (2)$$

where ρ_0 is the initial density, P_0 is the initial pressure, and ρ/ρ_0 is the compression.[16] Equations (1) and (2) are two of the Hugoniot relations (a third relation, which entails conservation of energy, was not considered).

Temperature is not a quantity in the Hugoniot relations. In an experiment to obtain data on the Hugoniot, the change in internal energy can be determined, but the partition of energy, and thus the temperature, cannot. Separate measurements are required to determine temperatures of shocked matter.

Early EOS experiments on H_2 and D_2 [Ref. 13] were well described by a model that neglected molecular dissociation.[6] However, recent measurements revealed a significantly lower temperature than predicted for pressures greater than 0.2 Mbar.[14] This was interpreted as dissociation of the molecular fluid at high density and temperature. A new model, referred to subsequently as the dissociation model, was formulated to incorporate this effect.[14] The dissociation model is not an *ab initio* theory; it is based on the ideal mixing of molecular states (using a soft-sphere perturbation theory) and monatomic states (using a one-component plasma model) and includes a single adjustable parameter set to agree with all shock-wave and shock-temperature data for H_2 and D_2.[13,14] The inclusion of molecular dissociation leads to a prediction of the compressibility, in the 0.2-Mbar to 5.0-Mbar pressure regime, that is significantly higher than that of the earlier model.[6] For example, the density of D_2 on the Hugoniot at 1.0 Mbar is 50% greater than calculated from the earlier model[6] and from the D_2 table included in the widely used Sesame EOS library.[17]

Equation of State Measurements Using Lasers

It has long been known that lasers are capable of driving very strong shocks into targets.[18] However, the production of EOS data in the megabar regime using lasers with uncertainties of less than 10% is virtually nonexistent. There are four challenges that must be confronted when attempting such experiments.

1. The shock produced must be spatially uniform. A modulated shock has a range of pressures and densities along the shock front; this is unsuitable for measurements. This issue can be addressed by target design and smoothing of the beam.[19] The shock should also be planar; producing a strong shock with a laser of high intensity obtained by focusing to a small spot may succeed only in driving a spherical, rather than planar, shock wave into the target, thus making difficult interpretation of the experiment. A laser spot that is too small will also be subject to edge effects; i.e., rarefaction waves releasing from the perimeter of the spot and moving radially inward. If the spot diameter is small, these rarefactions can reach the center of the spot on the timescale of the measurements, thus compromising the results.
2. The shock should be steady in time. A constant drive will produce a shock moving at a constant speed; e.g., a declining drive produces a decaying shock that must be characterized carefully. As will be shown subsequently, a constant

shock speed offers the possibility of obtaining data with small uncertainties.

3. Preheat has always been a concern in laser-produced EOS measurements. Penetrating x rays or hot electrons produced in the laser-interaction region (generally near 1 keV in temperature) can be absorbed in the sample being measured prior to the sample being shocked. The result is a change in the initial conditions of the sample, including the initial density ρ_0. Because measurements of the Hugoniot determine compression (ρ/ρ_0) rather than the final density (see Eq. 2), a change in ρ_0 means an error in the final density.
4. Typical spatial scales for megabar-regime laser experiments are micrometers, and timescales are a few tens of picoseconds. The diameter of the Nova laser spot used in the described experiment was less than 1 mm, and typical shock speeds in the deuterium were 30 km/s. Instrumentation and diagnostics appropriate for conditions such as these are necessary to produce meaningful data.

All of these challenges were addressed in the experiments described herein; hence, there is considerable confidence in the results.

Nova Experiments to Measure the EOS of Liquid Deuterium

To obtain absolute EOS data, we compressed liquid D_2 with a Nova-laser-driven shock wave launched from an Al pusher. Using temporally resolved radiography, we followed the propagation of the Al/D_2 interface and the shock front in the D_2 and measured the pusher speed, shock speed, and compression. We then determined the pressure by using Eq. (1).

A schematic of the cryogenic target cell is shown in Figure 1. Liquid D_2 was contained in a 1-mm-diam, 0.45-mm-long cylindrical cell machined into a Cu block. One end of the cell was sealed with an Al disk that served as the shock pusher; the opposite end of the cell was sealed with a 0.5-mm-thick sapphire window. The pusher was 100, 180, or 250 μm thick, depending on the experiment, and had a rear-side mean surface roughness of 30 nm rms. The pusher was coated with 15 to 25 μm of polystyrene external to the cell, and the polystyrene was overcoated with a 100-nm layer of Al. The thickness of the polystyrene layer was chosen to prevent direct laser ablation of the Al pusher, thus minimizing x-ray emission and consequent preheat of the pusher from x rays produced in the plasma. The Al overcoating eliminated direct optical laser shine through the plastic at onset of the laser pulse before an absorbing plasma formed. To accommodate radiography through the sides of the cell, a 500-μm-diam window was drilled into each side of the cell and sealed with a 5-μm-thick Be foil.

Liquid D_2 requires temperatures of approximately 20 K, so a cryostat was constructed for the two-beam facility at Nova, making this series the first cryogenic experiments ever fielded on Nova. The D_2 was loaded into the cell and pressurized to a few hundred torr. Temperatures were monitored to within 0.05 K. D_2 densities were determined from the saturation curve[20] and varied between 0.170 and 0.172 g/cm^3. The initial density ρ_0 for each experiment was known with an uncertainty of less than 0.1%.

One beam of the Nova laser (λ = 527 nm) was focused onto the target. Ablation of the polystyrene layer drove a shock wave through the Al and into the D_2. Side-on radiography of the D_2 revealed propagation of the Al/D_2 interface and the shock front. To ensure a spatially planar and uniform shock front, a kinoform phase plate[21] was inserted into the Nova beam to generate a smooth laser irradiance profile. The laser spot at the target plane was elliptical, with major and minor diameters as great as 900 and 600 μm, respectively, depending on focusing. Drive irradiances ranged from 5×10^{12} to 2×10^{14} W/cm^2. The Nova drive beam had an 8- or 10-ns temporally square profile with a rise time of 100 ps.

The results of the measurement depend on knowing the initial state of the D_2 (i.e., ρ_0) prior to shock arrival. This made it necessary to determine the preheat level of the pusher/D_2 interface at the time the shock arrived. The position of the rear pusher surface was monitored, with a Michelson interferometer,

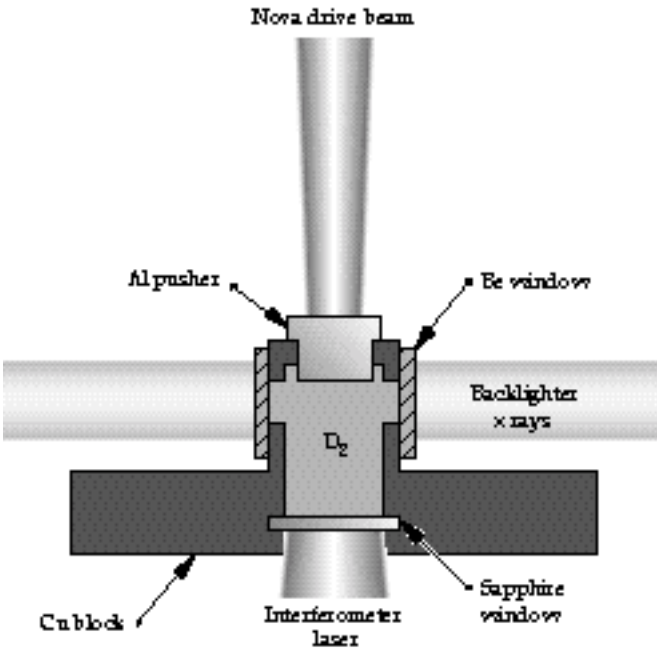

FIGURE 1. Schematic diagram of a cryogenic cell for laser-driven shock compression of liquid D_2. (08-00-0197-0007pb01)

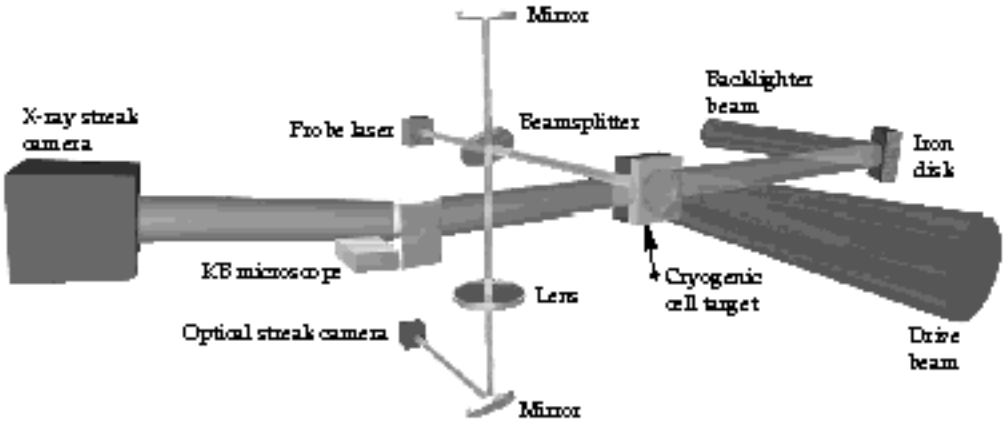

FIGURE 2. Schematic diagram of the experimental setup for simultaneous side-on radiography and end-on interferometry of a cryogenic cell with three laser beams: a smoothed Nova beam to drive a shock in the cell; an oppositely directed Nova beam to provide an x-ray backlighter; and a probe beam for the interferometer. (70-00-0297-0250pb01)

through the sapphire window. This provided the additional advantage of verifying the planarity of the shock at breakout. The interferometer-probe beam was a 10-ns-FWHM, 355-nm laser pulse appropriately time-delayed from the Nova drive beam that generated the shock wave. (The interferometer and results from the diagnostic are described in an article by K. S. Budil on page 11 of this *Quarterly*.) Using this instrument, we were able to confirm that the shock front in the D_2 was sufficiently planar for measurements and that the preheat levels in the D_2 were negligible. The arrangement for the experiment is shown in Figure 2.

Streaked radiography of the shocked D_2 was performed using a plasma x-ray source produced by focusing a second beam of Nova onto an Fe disk (10 ns at 6×10^{13} W/cm^2). The backlighter was placed 12 cm from the target cell to eliminate possible heating of the cell by the backlighter plasma. At that distance, the backlighter x rays produced a near-collimated source. The effective source size in the imaging direction was approximately 150 μm and was set by the width of the laser focal spot. Using the interferometer, we observed that the x-ray backlighter had no effect on the D_2 in the cell. X rays transmitted through the target cell were imaged by a Kirkpatrick–Baez (K-B) microscope onto a streak camera. The K-B microscope's bandpass was 750–840 eV, and the collection half-angle was 2.5 mrad. Two calibrated magnifications were used: 33× and 82×. The resolution of the K-B microscope in this geometry was found to be better than 3 μm over a 300-μm-wide field of view. The microscope imaged a strip 300 μm long by 5 to 30 μm high, depending on magnification and configuration.

An example of a streaked radiograph of shock-compressed D_2 is shown in Figure 3. The drive irradiance was 10^{14} W/cm^2 over 8 ns. The bright area in the figure is the view through the side windows of the cell. Because the pusher is opaque and the liquid transparent, the Al/D_2 interface is the boundary between the light and dark regions. In the figure, the interface is stationary prior to 2 ns. At 2 ns, the laser-driven shock crosses the interface, and the pusher surface accelerates to a steady speed (the particle speed). A shock front can be seen moving ahead of the interface as the shock wave is driven into the D_2. The shock front, which appears as the dark line, is made visible because of refraction of backlighter x rays at the density jump across the shock front. X rays grazing the shock-front interface are refracted to angular deflections greater than 2.5 mrad and, therefore, out of the angular field of the K-B microscope (x rays impinging at nongrazing angles are internally reflected, so there is transmission between the Al/D_2 interface and the shock front). The detection of the shock front by refraction is similar to the Schlieren technique for detecting density gradients. The steady propagation of both the shock front and the interface is demonstrated by their linear trajectories until ~6 ns, when a stronger shock enters the D_2. The second shock is caused by shock reverberations in the pusher. (In this example, no data after 6 ns were used.) The shock and particle speeds U_s and U_p can be evaluated from the slopes.

The single shock compression can be determined by Eq. (2) using the individually derived shock and pusher speeds. It also can be measured directly from

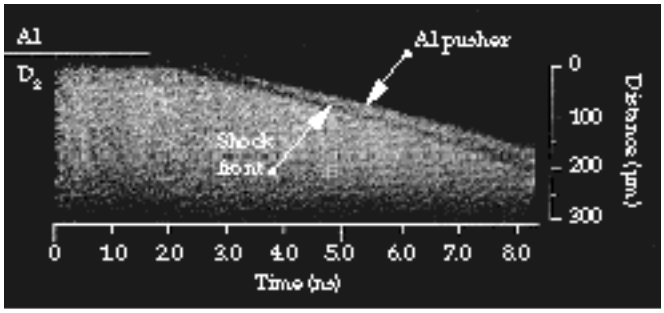

FIGURE 3. A time-resolved, side-on radiograph of a laser-shocked D_2 cell. The bright area views the D_2 through Be windows bounded by the x-ray-opaque Al pusher above. The pusher is seen advancing after breakout at 2 ns; the shock is the dark line in front of and moving faster than the pusher–D_2 interface. (70-00-0297-0249pb01)

the film as long as U_s and U_p are constant (in the experiments, U_s and U_p were constant to better than 1%). At any time t, the compression is equal to the ratio of two lengths: the distance between the shock front $X_2(t)$ and the initial interface position X_0, which is the thickness of a layer of uncompressed D_2, and the distance between the shock front and the interface $X_1(t)$, which is the thickness of the now-compressed layer. Thus $\rho/\rho_0 = [X_2(t) - X_0]/[X_2(t) - X_1(t)]$. Because all of the measurements are made on one piece of film in the streak camera, uncertainties in ρ/ρ_0 due to magnification and sweep speed are canceled in this ratio. In the experiments, we observed a steady shock for 4 to 8 ns with no measurable change in speed of the Al/D_2 interface. Comparison with Eq. (2) provides an internal consistency check on ρ/ρ_0.

The shock position that we observed in the radiograph is the leading part of the shock front that emerged from the center of the pusher. In some experiments, the apparent Al/D_2 interface position at $t = 0$ on film was not identical to the actual value of X_0 because the rotation of the cell about the axis perpendicular to both the backlighter path and the shock path (the axis looking into the page in Figure 1) could be controlled only to within 3 mrad. This resulted in the center of the pusher being shadowed by an edge of the pusher before the shock front emerged from the pusher. In these cases, the shock and interface trajectories did not converge on the film. Extrapolation of the trajectories, however, revealed X_0 as the intersection of the two paths. Alternatively, shock and interface positions taken at two different times were used to determine X_0. This resulted in correcting, by as much as 10%, the compression obtained using the *apparent* position X_0 on film and increased the uncertainty in ρ/ρ_0 from approximately ±3% to approximately ±5%.

The Al/D_2 interface is subject to the Richtmyer–Meshkov hydrodynamic instability (RM). However, using the measured pusher finish of 30 nm, we calculated that the largest perturbation expected from RM is less than 0.5 μm during the times of observation, approximately 1% to 2% of the compression.

Figure 4 shows the pressures and final densities determined from the known initial densities and measured compressions. As explained previously, the error bars are governed predominantly by accuracy in determining the slopes of the shock and interface trajectories in the radiographs. The figure plots curves of the Hugoniot from the dissociation model[14] and the Sesame EOS table.[17] The gas-gun observations[13] are also shown. At the lowest compression, our data are in agreement with the earlier results; at higher compressions, the data deviate from the Sesame prediction. The data point at 0.25 Mbar is significant because it overlies the more accurate gas-gun data,

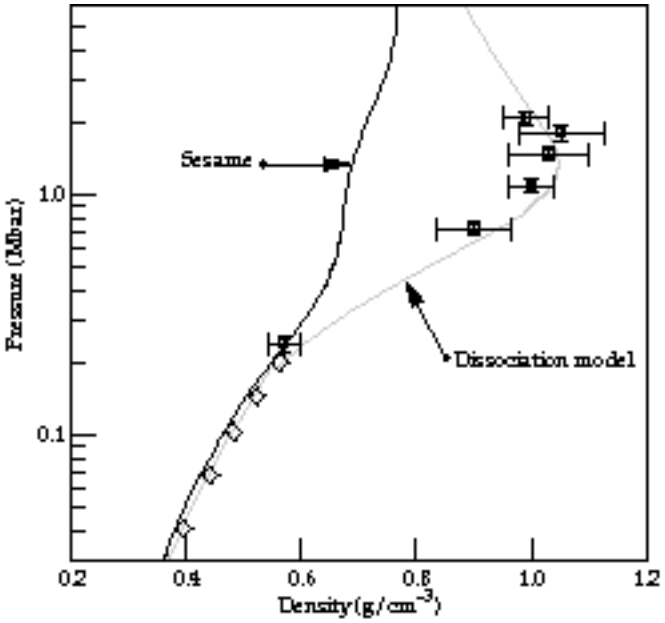

FIGURE 4. The measured data are shown as squares with error bars compared with Hugoniots derived from the Sesame EOS library,[17] which is similar to an EOS without dissociation,[6] and the proposed dissociation model of Ref. 14. The diamond shapes depict gas-gun data.[13] (70-00-0297-0248pb01)

lending confidence to our results. The laser data evince an enhanced compressibility comparable to that of the dissociation model in the region where occurrence of strong dissociation was predicted. We conclude from this that molecular dissociation is indeed significant in hydrogen isotopes compressed near 1.0 Mbar.

Conclusion

These are the first measurements of the density, shock speed, and particle speed in D_2at pressures greater than 0.2 Mbar. The range of pressures measured extended from 0.25 to 2.1 Mbar, encompassing the regime of the first shock prescribed by the NIF point-design ignition capsule. These absolute data of Hugoniot strongly indicate a dissociative transition from the diatomic to the monatomic fluid state. Because an accurate model of the dissociation was not incorporated in previous EOS theories for hydrogen, the data provide an important benchmark for a revised theory for hydrogen and its isotopes in a regime relevant to high-energy-density physics and ICF. The more compressible EOS of hydrogen indicated by these data offers higher performance and improved margin for NIF ignition capsules. Finally, the experiments demonstrate that laser-driven shocks can effectively and confidently be used for EOS studies at pressures beyond those attainable by traditional techniques.

Acknowledgments

The authors would like to thank R. M. More, F. J. Rogers, M. Ross, D. A. Young, and J. D. Johnson (Los Alamos National Laboratory) for advice on the theory and S. N. Dixit for designing the kinoform phase plate.

Notes and References

1. S. Ichimaru, H. Iyetomi, and S. Tanaka, *Phys. Rep.* **149,** 91 (1987).
2. N. W. Ashcroft, *Phys. World* **8** (7), 43 (1995).
3. R. Smoluchowski, *Nature* **215,** 691 (1967); V. N. Zharkov and V. P. Trubitsyn, *Jupiter,* T. Gehrels, Ed. (University of Arizona Press, Tucson, 1976), pp. 135–175; W. B. Hubbard, *Science* **214,** 145 (1981); W. J. Nellis, M. Ross, and N. C. Holmes, *Science* **269,** 1249 (1995).
4. J. D. Lindl, *Phys. Plasmas* **2,** 3933 (1995).
5. W. B. Hubbard, *Astrophys. J.* **152,** 745 (1968).
6. M. Ross, F. H. Ree, and D. A. Young, *J. Chem. Phys.* **79,** 1487 (1983).
7. D. Saumon, G. Chabrier, and H. M. Van Horn, *Astrophys. J. Supp.* **99,** 713 (1995).
8. W. R. Magro, D. M. Ceperley, C. Pierleoni, and B. Bernu, *Phys. Rev. Lett.* **76,** 1240 (1996).
9. S. W. Haan, S. M. Pollaine, J. D. Lindl, L. J. Suter, et al., *Phys. Plas.* **2,** 2480 (1995); W. J. Krauser, N. M. Hoffman, D. C. Wilson, B. H. Wilde, et al., *Phys. Plas.* **3,** 2084 (1996).
10. S. W. Haan, LLNL Y Division, Livermore, CA, private communication (August 1995).
11. L. B. Da Silva, P. Celliers, G. W. Collins, K. S. Budil, et al., "Absolute Equation-of-State Measurements of Shocked Liquid Deuterium up to 200 Gpa (2 Mbar)," to appear in *Phys. Rev. Lett.* (1997).
12. H. K. Mao and R. J. Hemley, *Rev. Mod. Phys.* **66,** 671 (1994).
13. W. J. Nellis, A. C. Mitchell, M. van Theil, G. J. Devine, et al., *J. Chem. Phys.* **79,** 1480 (1983).
14. N. C. Holmes, M. Ross, and W. J. Nellis, *Phys. Rev. B* **52,** 15835 (1995).
15. S. T. Weir, A. C. Mitchell, and W. J. Nellis, *Phys. Rev. Lett.* **76,** 1860 (1996).
16. Y. B. Zel'dovich and Y. P. Raizer, *Physics of Shock Waves and High-Temperature Hydrodynamic Phenomena* (Academic Press, New York, 1966).
17. G. I. Kerley, *A Theoretical Equation of State for Deuterium*, Los Alamos Scientific Laboratory Report LA-4776 (New Mexico, January 1972).
18. R. J. Trainor, J. W. Shaner, J. M. Auerbach, and N. C. Holmes, *Phys. Rev. Lett.* **42,** 1154 (1979).
19. R. Cauble, L. B. Da Silva, S. G. Glendinning, S. M. Lane, et al., *Inertial Confinement Fusion, 1993 ICF Annual Report,* Lawrence Livermore National Laboratory, Livermore, CA, UCRL-LR-105820-93, 131–136 (1994).
20. P. C. Souers, *Hydrogen Properties for Fusion Energy* (University of California Press, Berkeley, 1986).
21. S. N. Dixit, M. D. Feit, M. D. Perry and H. T. Powell, *Opt. Lett.* **21**, 1715 (1996).